JCB Article

Sim4: a novel fission yeast kinetochore protein required for centromeric silencing and chromosome segregation

Alison L. Pidoux,[1,2] William Richardson,[2] and Robin C. Allshire[1,2]

[1]Wellcome Trust Centre for Cell Biology, Institute of Cell and Molecular Biology, University of Edinburgh, Edinburgh EH9 3JR, UK
[2]Medical Research Council Human Genetics Unit, Western General Hospital, Edinburgh EH4 2XU, UK

Fission yeast centromeres are composed of two domains: the central core and the outer repeats. Although both regions are required for full centromere function, the central core has a distinct chromatin structure and is likely to underlie the kinetochore itself, as it is associated with centromere-specific proteins. Genes placed within either region are transcriptionally silenced, reflecting the formation of a functional kinetochore complex and flanking centromeric heterochromatin. Here, transcriptional silencing was exploited to identify components involved in central core silencing and kinetochore assembly or structure. The resulting *sim* (silencing in the middle of the centromere) mutants display severe chromosome segregation defects. *sim2*$^+$ encodes a known kinetochore protein, the centromere-specific histone H3 variant Cnp1$^{CENP\text{-}A}$. *sim4*$^+$ encodes a novel essential coiled-coil protein, which is specifically associated with the central core region and is required for the unusual chromatin structure of this region. Sim4 coimmunoprecipitates with the central core component Mis6 and, like Mis6, affects Cnp1$^{CENP\text{-}A}$ association with the central domain. Functional Mis6 is required for Sim4 localization at the kinetochore. Our analyses illustrate the fundamental link between silencing, chromatin structure, and kinetochore function, and establish defective silencing as a powerful approach for identifying proteins required to build a functional kinetochore.

Introduction

The centromere is the chromosomal site at which the kinetochore assembles. Kinetochores interact with microtubules (MTs)* of the mitotic and meiotic spindles and ensure the equal segregation of chromosomes at cell division (Pidoux and Allshire, 2000a; McIntosh et al., 2002; Nasmyth, 2002). Centromeres must replicate but remain linked until anaphase. The resulting sister centromeres must be bioriented with all MT-binding sites of each kinetochore facing the same direction to promote proper bilateral spindle interactions. Congression of chromosomes to the metaphase plate and their movement to opposite poles require MT dynamics and MT motor proteins acting at the kinetochores. The kinetochore is a monitoring and effector site for the spindle checkpoint (Musacchio and Hardwick, 2002). An active centromere is also responsible for its own propagation; epigenetic mechanisms based on protein heritability and protein modifications contribute to the maintenance of the site of centromere activity (Karpen and Allshire, 1997; Sullivan et al., 2001).

Understanding these kinetochore properties requires the identification of its protein components. The kinetochore consists of a very large complex of many proteins even in simple organisms (He et al., 2001; Cheeseman et al., 2002). The fission yeast, *Schizosaccharomyces pombe*, provides an excellent system for the investigation of centromere–kinetochore function because it combines genetic tractability with structurally complex centromeres (Pidoux and Allshire, 2000b). The three fission yeast centromeres share the same structural organization (Fig. 1 A; Hahnenberger et al., 1991; Takahashi et al., 1992; Pidoux and Allshire, 2000b). At each centromere, a central core region (*cnt*) is surrounded by inverted repeat elements (innermost repeats; *imr*), which are specific to each centromere. These are flanked by the outer

The online version of this article includes supplemental material.

Address correspondence to Robin C. Allshire, Wellcome Trust Centre for Cell Biology, Institute of Cell and Molecular Biology, 6.34 Swann Building, University of Edinburgh, Mayfield Road, Edinburgh EH9 3JR, UK. Tel.: 44-131-650-7117. Fax: 44-131-650-7778. E-mail: robin.allshire@ed.ac.uk

*Abbreviations used in this paper: ChIP, chromatin immunoprecipitation; IP, immunoprecipitate; MNase, micrococcal nuclease; MT, microtubule; TBZ, thiabendazole.

Key words: kinetochore; chromatin; centromere; silencing; chromosome segregation

© The Rockefeller University Press, 0021-9525/2003/04/295/13 $8.00

The Journal of Cell Biology

repeat elements (*otr*), the organization of which differs between the three centromeres. The central cores of *cen1* and *cen3* share a 4-kb element, *cnt1*/*cnt3*, which is partially conserved in *cen2* (Wood et al., 2002).

The central region (including the inner part of the *imr* sequences) and the outer repeat regions form two distinct domains (Fig. 1 A). The outer repeats are assembled in chromatin, which resembles centromeric heterochromatin in metazoa. Genes placed within fission yeast centromeres are transcriptionally silenced (Allshire et al., 1994, 1995), and this is likely to reflect packaging into heterochromatin and the assembly of the kinetochore complex. Several mutants have been identified that alleviate transcriptional silencing and concomitantly affect centromere function (Allshire et al., 1995; Ekwall et al., 1995, 1997; Partridge et al., 2000). Most of these affect only the heterochromatic *otr* domain and include mutants in *swi6*$^+$, which encodes a chromodomain protein (HP1 homologue; Ekwall et al., 1995), *clr4*$^+$, which encodes a histone methyltransferase (Rea et al., 2000), and *rik1*$^+$. The only mutants shown to strongly alleviate central core silencing are *mis6* and *mal2*, and they do not alleviate *otr* silencing (Partridge et al., 2000; Jin et al., 2002). The existence of two classes of mutants is reflected in the regions of centromeric DNA with which the encoded proteins associate (Partridge et al., 2000). Swi6 and Chp1 are specifically associated with the *otr* region, whereas Mis6 and Mal2 associate with the central core region (Saitoh et al., 1997; Partridge et al., 2000; Jin et al., 2002). Ultrastructural studies also reveal two physically distinct domains (Kniola et al., 2001).

Nucleosomes of the outer repeats, like other heterochromatin, are underacetylated on histone H3 and H4 tails (Ekwall et al., 1997) and methylated on lysine 9 of H3. Recent observations suggest a model in which Clr4, guided by RNAi activity, methylates histone H3, promoting Swi6 binding and the assembly of transcriptionally silent heterochromatin (Bannister et al., 2001; Nakayama et al., 2001; Partridge et al., 2002; Volpe et al., 2002, 2003), which is required for the recruitment of a high density of Rad21-cohesin to the centromere (Bernard et al., 2001; Nonaka et al., 2002).

Central core chromatin is unusual; limited digestion with micrococcal nuclease (MNase) generates a smear rather than a nucleosomal ladder typical of most chromatin (Polizzi and Clarke, 1991; Takahashi et al., 1992). Mutants in central core–associated proteins disrupt this central core–specific chromatin structure (Saitoh et al., 1997; Goshima et al., 1999; Takahashi et al., 2000; Jin et al., 2002). The composition of central core chromatin is also distinct, as evidenced by the specific association of the H3 variant Cnp1 (fission yeast CENP-A; Takahashi et al., 2000). Mis6 is required for the incorporation of newly synthesized Cnp1–GFP at centromeres (Takahashi et al., 2000). It is likely that the "kinetochore proper" assembles at the central core, and the outer repeats provide an important but auxiliary role, possibly affecting kinetochore conformation in addition to centromeric cohesion. In support of such a model, the MT-associated protein Dis1 is associated with the central core region in a mitosis-specific manner (Nakaseko et al., 2001). However, another MAP, Alp14/Mtc1, associates with *otr* and *imr* in mitosis, but not with *cnt* (Garcia et al., 2001; Nakaseko et al., 2001). Each fission yeast kinetochore, like those of many metazoa, contains multiple MT-binding sites (Ding et al., 1993). In contrast, budding yeast centromeres associate with one MT (Winey et al., 1995). An additional level of organization must operate at the more complex kinetochores so that all MT attachment sites are oriented in a concerted fashion toward the same pole.

Metazoan kinetochores are not easily dissected by genetic screens, and much knowledge has stemmed from the use of autoimmune sera (Pluta et al., 1995). An alternative route to the identification of mammalian kinetochore proteins is by homology to proteins discovered in genetically tractable organisms (Wigge and Kilmartin, 2001; Nishihashi et al., 2002). Screens based on minichromosome stability performed in budding and fission yeasts have garnered mutants affecting cohesion, replication, as well as kinetochore function (for review see Pidoux and Allshire, 2000b).

The phenomenon of silencing at fission yeast centromeres sets them apart from those of budding yeast and provides an effective tool for the direct identification of kinetochore components. We have exploited transcriptional silencing at fission yeast centromeres to isolate mutants that affect centromere function, chromatin structure, and chromosome segregation. The identification of *sim2*$^+$ as Cnp1$^{CENP\text{-}A}$ validates this approach. A novel kinetochore protein, Sim4, has also been identified and shown to be associated with the centromere central core region, and to form a complex with the central core component Mis6.

Results

A sensitive assay to monitor central core silencing

Transcription is more weakly repressed in the central core (*cnt*) compared with the outer repeat regions (*otr*) of fission yeast centromeres (Allshire et al., 1994); insertion of the *ura4*$^+$ gene in the central core of *cen1* (*cnt1:ura4*) allows good growth on medium lacking uracil, giving an unacceptable background for screening. To overcome this, a promoter-crippled *arg3*$^+$ gene was inserted into *cnt1* (Fig. 1 A). Strains containing *cnt1:arg3* grew very slowly on media lacking arginine (−arg), forming tiny colonies after several days incubation at 25°C (Fig.1 C). As predicted, the *mis6* mutant (Saitoh et al., 1997; Partridge et al., 2000) alleviated central core silencing and allowed fast growth on −arg medium, whereas mutations in the *rik1*$^+$ gene, required for outer repeat and telomeric silencing (Allshire et al., 1995), had little effect (Fig. 1 C). Thus the *cnt1:arg3* insertion provided sufficient sensitivity and specificity to be usable in a genetic screen. To monitor silencing at other sites, strains were constructed with the genotype *cnt1:arg3 otr2:ura4 cnt3:ade6 tel1L:his3*$^+$ (Fig. 1 B; Allshire et al., 1994, 1995; Nimmo et al., 1998). The *ura4*$^+$ and *his3*$^+$ genes are strongly silenced at *otr2* and the telomere, respectively (Fig. 1 C); the *cnt3:ade6* insertion proved not to be useful for screening purposes. Strains with this genotype were designated FY3027 and FY3033 and will be henceforth referred to as wild type.

Isolation of mutants that alleviate central core silencing

Wild-type strains were mutagenized (Fig. 1 B) and fast-growing arg+ colonies picked (Fig. 1 C). Because genes en-

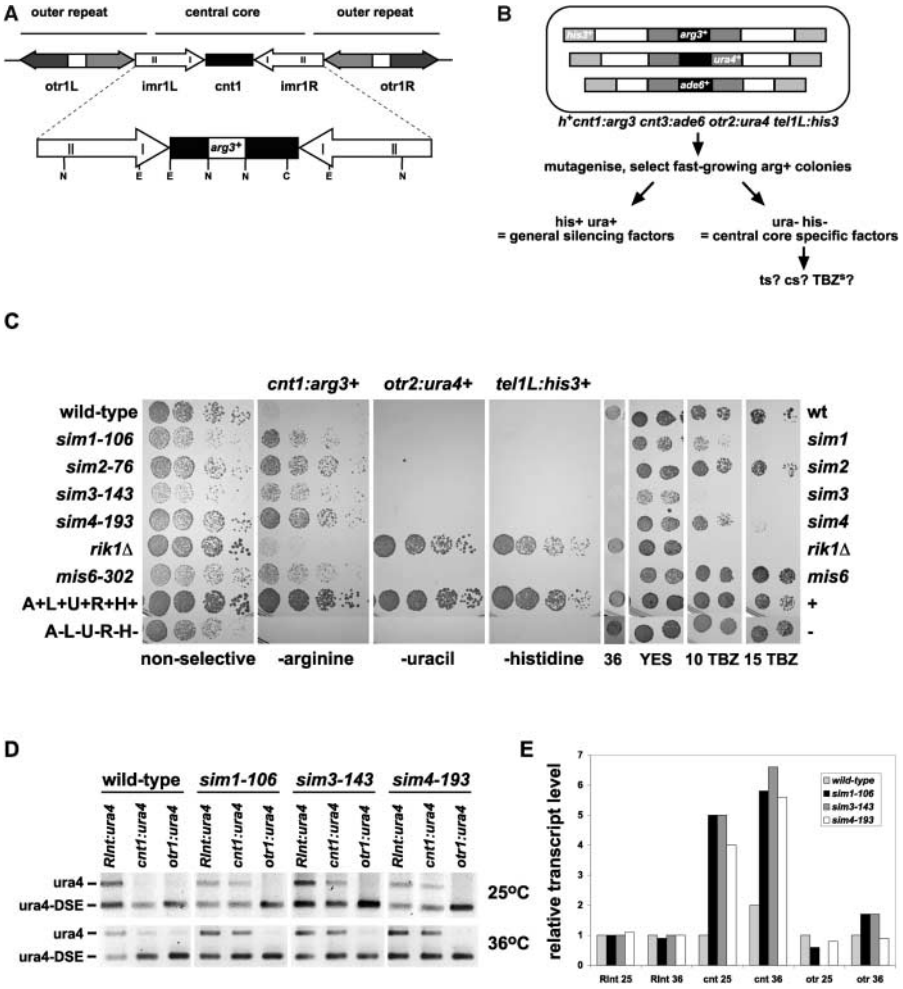

Figure 1. **A genetic screen to identify mutants that alleviate silencing in the centromere central core.** (A) *S. pombe* centromere 1. (Top) Central core (*cnt1* and inner part of *imr1L* and *imr1R*) surrounded by outer repeat regions (*otr*). Vertical lines indicate the position of tRNA genes at the transition point between the two domains (Partridge et al., 2000). (Bottom) Structure of the *arg3*$^+$ insertion at the central core. Restriction sites: N, NcoI; C, ClaI; E, EcoRI. (B) Diagram of strain FY3027 used to isolate mutants defective in central core silencing, showing insertion sites of marker genes used to assay silencing. (C) Serial dilutions of *S. pombe* strains to assay silencing at various loci. The first spot contains 5 × 10^3 cells followed by fivefold dilutions. Plates were incubated at 25°C for 3–7 d. Assessment of growth on YES at 36°C and YES containing 0, 10, or 15 mg/ml TBZ at 25°C. (D) RT-PCR of *ura4* transcripts from random integrant (*Rint*), *cnt1*, and *otr1* insertion sites, compared with a *ura4* minigene control (*ura4-DSE*) at the endogenous locus. Strains analyzed were FY4835, 4837, 4841, 5711, 5717, 5674, 5695, 5719, 5683, 5714, 5720, and 5688. (E) Quantification of RT-PCR shown in D. The levels of transcripts normalized to *ura4-DSE* are expressed relative to the wild type at 25°C for each *ura4*$^+$ insertion site, *Rint*, *cnt1*, and *otr1*.

coding central core–associated proteins are essential, we screened for conditional lethality: 55 of 180 mutants were thermo- or cryosensitive and/or sensitive to the MT-disrupting drug thiabendazole (TBZ). 17 of the conditional lethal mutants were placed into four complementation groups, *sim1*, *2*, *3*, and *4*, for silencing in the middle of the centromere (see Fig. S1, available at http://www.jcb.org/cgi/content/full/jcb.200212110/DC1). These mutants alleviated silencing at *cnt1:arg3* but maintained silencing at *otr* and the telomere (Fig. 1 C). None of the *sim* mutants are allelic to *mis6*$^+$, *mis12*$^+$, or *mal2*$^+$, which are known, or predicted, to alleviate central core silencing (Saitoh et al., 1997; Goshima et al., 1999; Partridge et al., 2000; Jin et al., 2002). *sim2*$^+$ is allelic to *cnp1*$^{CENP\text{-}A}$ (Takahashi et al., 2000; Mellone, B.G., personal communication).

To quantify defective centromere silencing, *sim* mutant strains with the *ura4*$^+$ gene inserted at either *cnt1*, *otr1*, or a random integrant euchromatic control locus (*Rint*) and a *ura4* minigene control (*ura4-DSE*) at the endogenous *ura4*$^+$ locus (Allshire et al., 1994; Partridge et al., 2000) were analyzed by RT-PCR. There was a significant increase in *ura4*$^+$ message from the *cnt1:ura4* site in *sim* mutants compared with wild type at permissive and restrictive temperatures (Fig. 1, D and E). Little or no alleviation of silencing was observed at *otr1:ura4*. These data confirm that the alleviation of silencing in *sim* mutants was specific to the central core region.

sim mutants display severe defects in chromosome segregation

sim mutants showed enhanced loss rates of a minichromosome (Fig. S1). *sim1*, *sim3*, and *sim4* showed greater sensitivity to TBZ than wild type, but lower sensitivity than *otr* mutants such as *rik1*, *clr4*, and *swi6* (Fig. 1 C; Ekwall et al., 1996). Neither *sim2* nor *mis6* showed supersensitivity to TBZ. To investigate the chromosome segregation defects, *sim* mutants were grown at permissive (25°C) or restrictive temperature (36°C for 6 h), fixed, and processed for immunofluorescence with α-tubulin antibody. *sim1*, *3*, and *4* displayed lagging chromosomes on late anaphase spindles (Fig. 2, B–D) and uneven segregation of chromosomes. Short spindles with hypercondensed chromatin were common. Star or V-shaped spindles were seen frequently in *sim3* mutants, which may indicate defects in the organization of a bipolar spindle.

The *sim4* mutant was analyzed in greater detail (Fig. 2 E). There was a high proportion of cells with short spindles with hypercondensed chromosomes, rarely seen in wild-type cells. 36% of late anaphase cells showed apparently normal segregation, 24% had uneven segregation, and 40% showed lagging chromosomes. FISH performed with a probe that hybridizes to the ribosomal DNA repeats revealed all permutations of chromosome III segregation (Fig. 2 F). Uneven segregation and lagging chromosomes are seen in the

The Journal of Cell Biology

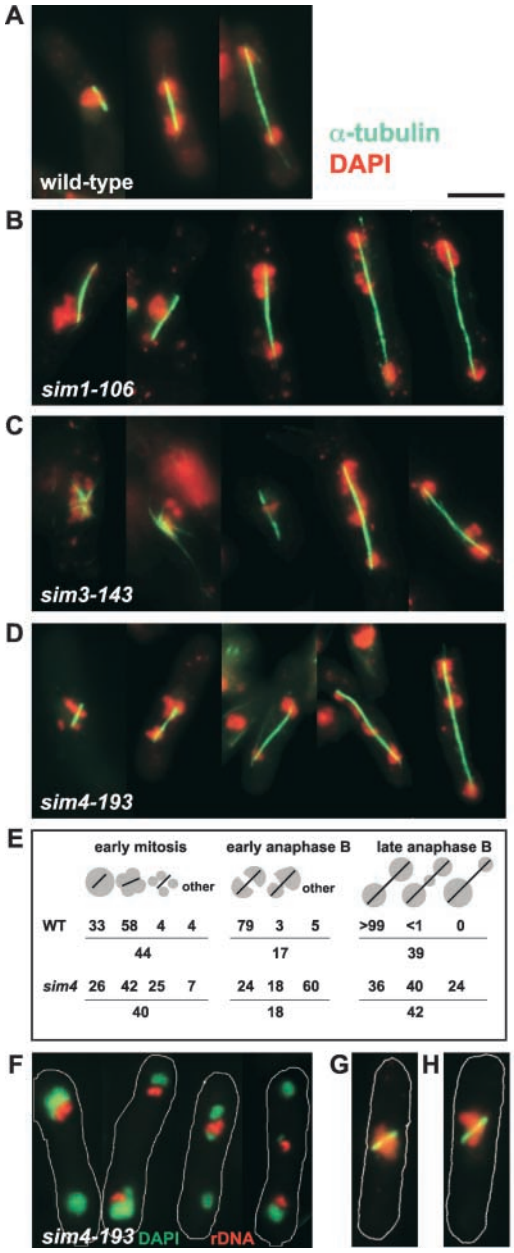

Figure 2. **Chromosome segregation defects in *sim* mutants.** (A–D) Strains (FY3027, 4484, 4502, and 4536) were shifted to 36°C for 6 h before fixation and immunofluorescence with TAT1 α-tubulin antibody (green) and DAPI staining of DNA (red). Bar, 5 μm. (A) Equal chromosome segregation in wild-type cells. (B) *sim1-106*, uneven segregation and lagging chromosomes. (C) *sim3-143*, similar phenotypes and star-shaped spindles (first two cells). (D) *sim4-193*, uneven segregation and lagging chromosomes. (E) Table of chromosome segregation phenotypes in wild type and the *sim4* mutant at restrictive temperature. The top set of numbers is the percentage of cells in that category (early mitosis [prometaphase, metaphase, anaphase A], early anaphase B, late anaphase B) that displayed the phenotype diagrammed. The bottom figures indicate the percentage each category makes to the total of mitotic cells. (F) FISH with a probe to the ribosomal DNA clusters on the ends of chromosome 3 (rDNA [red], DAPI [green]). (G and H) Spindle length in *cut9* (G) and *cut9sim4* (H) cells incubated at 36°C for 4 h (α-tubulin [green], DAPI [red]).

first mitosis after release from a G1 block, indicating that both are primary defects in *sim4* mutants (unpublished data). Preliminary observations suggest that *sim4* is not defective in centromeric cohesion, nor does it display the declustering of centromeres seen in *mis6* mutants (Saitoh et al., 1997). Mutants defective in kinetochore function have longer metaphase spindles than normal (Goshima et al., 1999; Jin et al., 2002); this is presumably due to reduced kinetochore-to-pole tension or to a defect in MT function. Spindle length was measured in metaphase-arrested *cut9* and *cut9sim4* cells that had been shifted to 36°C for 4 h (Fig. 2, G and H). There was a 13% increase in spindle length in *sim4cut9* (2.63 ± 0.94 μm) compared with *cut9* (2.32 ± 0.54 μm). Overexpression of the spindle checkpoint component Mad2 was used as an alternative method of blocking in metaphase (He et al., 1997). *sim4-193* cells showed a 12% increase in spindle length compared with wild type (2.68 ± 0.37 μm and 2.40 ± 0.31 μm, respectively). These observations suggest that the *sim4* mutant has defects in kinetochore–spindle interactions.

Central core chromatin structure is disrupted in the *sim4* mutant

Chromatin was analyzed by limited MNase digestion and hybridization with a *cnt1* probe. As shown in Fig. 3, the unique central core smear pattern seen in wild type (Polizzi and Clarke, 1991; Takahashi et al., 1992) was lost and replaced by a ladder in the *sim4* mutant at permissive and restrictive temperatures. Similar observations have been made in other strains that have defects in central core proteins (Saitoh et al., 1997; Goshima et al., 1999; Takahashi et al., 2000; Jin et al., 2002).

sim4$^+$ encodes a novel protein that localizes to centromeres

A genomic plasmid was isolated by complementation of the *sim4* temperature-sensitive phenotype. The *sim4* mutation is closely linked to the mating type locus, and the complementing genomic fragment is 35 kb from *mat2/mat3*. The *sim4-193* allele was found to have a mutation causing a methionine to lysine change at amino acid 230 in ORF O94494 (SPBC18E5.03c; Fig. S2, available at http://www.jcb.org/cgi/content/full/jcb.200212110/DC1). This ORF has therefore been designated *sim4*$^+$ and is predicted to encode a novel 31.7-kD protein with large regions of coiled coil (Fig. S2). The *sim4*$^+$ gene is essential (Fig. S2); *sim4Δ* spores from tetrad dissections germinated but divided only four to six times.

Antibodies were raised against GST–Sim4 and affinity purified. Western analysis of total *S. pombe* protein extracts revealed a band of ~30 kD (Fig. S2) that increased in intensity when Sim4 was expressed from a multicopy plasmid, and was replaced by an ~60-kD band in a strain with a *sim4*–GFP fusion gene at the *sim4*$^+$ locus (see below). Thus, the polyclonal antibodies are specific for Sim4. Western analysis showed that there was no change in the amount of Sim4 present in a *sim4* strain, indicating that its defect is not due to decreased protein stability (Fig. S2; unpublished data).

The *sim4*$^+$ ORF was COOH-terminally tagged at its genomic locus with GFP (Bahler et al., 1998). A single GFP spot was seen in the nucleus of living cells in interphase, reminiscent of clustered centromeres (Fig. 4 A). Several

The Journal of Cell Biology

The Journal of Cell Biology

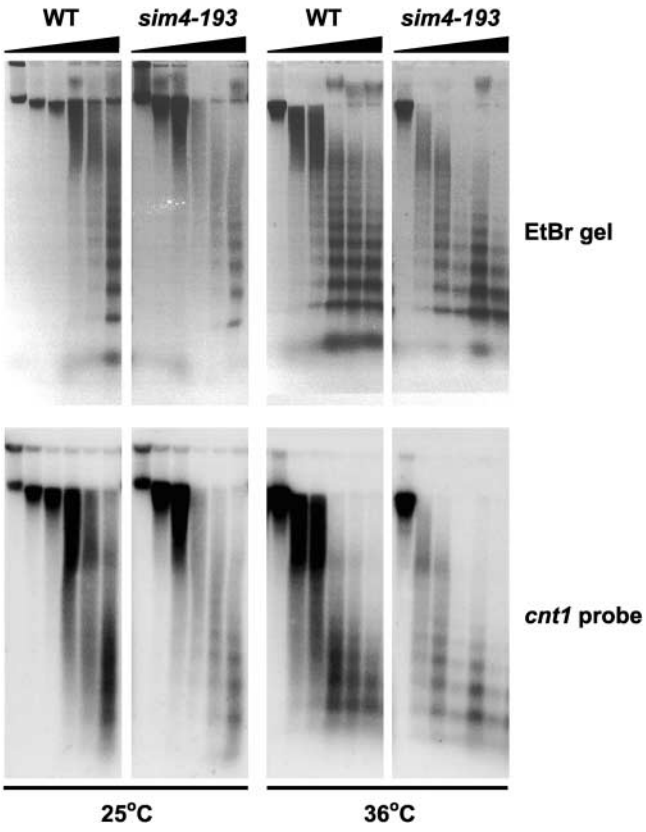

Figure 3. **Central core chromatin structure is disrupted in a *sim4* mutant.** MNase digestion of chromatin from cells (FY3027 and 4536) grown at 25°C or shifted to 36°C for 6 h. Top, ethidium bromide–stained gel with ladder indicative of partial MNase digestion. Bottom, Southern blot hybridized with *cnt1* probe, showing that the smear pattern in wild type is replaced by ladder-like pattern in the *sim4* mutant.

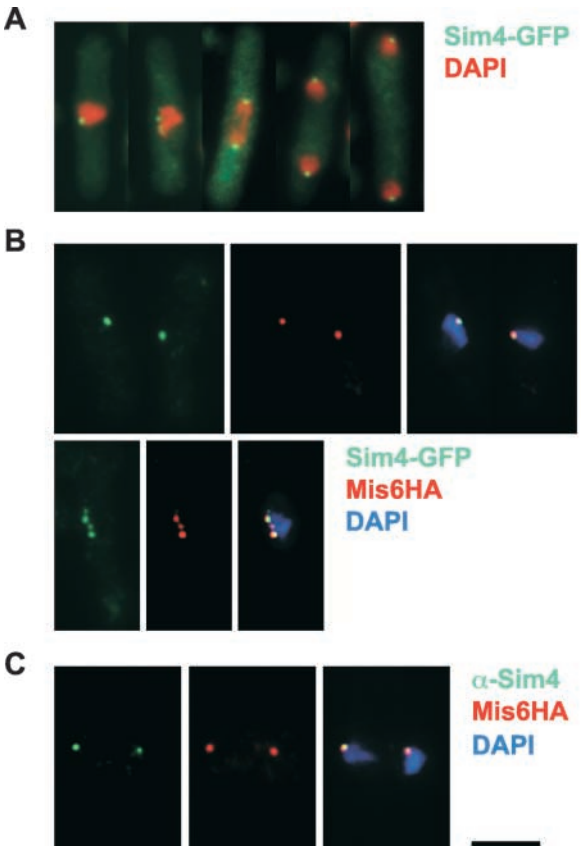

Figure 4. **Sim4 colocalizes with centromeres.** (A) Cells expressing Sim4–GFP (FY5077), showing from left to right: interphase (the three centromeres are clustered); early mitosis (prometaphase or metaphase or anaphase A), four centromeric spots are visible; early, mid, and late anaphase B (centromeres are at the spindle poles). (B) Colocalization of Sim4–GFP (green) with Mis6–HA (red) and merged image (right) in interphase (top row) and early mitosis (bottom row). Strain FY5237. (C) Colocalization of Sim4 (α-Sim4, green) with Mis6–HA (red), the merged image is shown on the right. Strain FY2929. Bar, 5 μm.

spots were seen in early mitotic cells, likely to be individual (or replicated) centromeres (Fig. 4, A and B); in anaphase B cells, spots were observed at the leading edges of the daughter nuclei (Fig. 4 A). Cells expressing both Sim4–GFP and Mis6–HA (Saitoh et al., 1997) were fixed and stained with α-GFP and α-HA antibodies, revealing colocalization of the two epitopes (Fig. 4 B). Colocalization of endogenous Sim4 and Mis6–HA was also observed (Fig. 4 C). Thus, the Sim4 localization pattern and colocalization with the bona fide kinetochore protein Mis6 indicate that Sim4 is a novel centromere-associated protein.

Sim4 is associated with the centromere central core region

To determine with which region(s) of the centromere Sim4 is associated, chromatin immunoprecipitation (ChIP) experiments were performed. DNA present in crude extracts and α-Sim4 ChIPs was analyzed using four primer pairs in a multiplex PCR. These primer pairs specifically amplify regions within the central core of *cen1* and *3* (*cnt*), the inner repeats of *cen1* (*imr*), the outer repeat of *cen1* (*otr*), and *fbp1*$^+$, a control euchromatic gene (*fbp*). As shown in Fig. 5 A, central core (*cnt*) sequences and inner repeat (*imr*) sequences were enriched 6.5- and 6.8-fold, respectively, relative to *fbp* in Sim4 ChIPs compared with the input control. Outer repeat sequences (*otr*) were not enriched. These experiments indicate that Sim4 is specifically associated with the central domain of the centromere but is absent from the outer repeat regions.

Several centromere-associated proteins, including Mis6 and Swi6, but not Chp1, have been shown to be capable of coating, or spreading over, noncentromeric DNA inserted in the fission yeast centromere (Partridge et al., 2000). To determine whether Sim4 is capable of coating exogenous DNA inserted at the central core, Sim4 ChIP was performed on a strain containing *ura4*$^+$ inserted at *cnt1*, and a control strain with *ura4*$^+$ at a control random integrant (*Rint*) euchromatic locus. Both strains also contained the *ura4* minigene control (*ura4-DSE*). There was no enrichment of *Rint:ura4* in Sim4 ChIPs, but *cnt1*:*ura4*$^+$ was enriched 11.9-fold compared with *ura4-DSE* (Fig. 5 B). As chromatin was sheared to an average of 500–1,000 bp, this enrichment was due to Sim4 assembled over *ura4*$^+$ sequences and not simply due to that on surrounding *cnt1* sequences. This confirms that Sim4 is associated with the central domain and also indicates

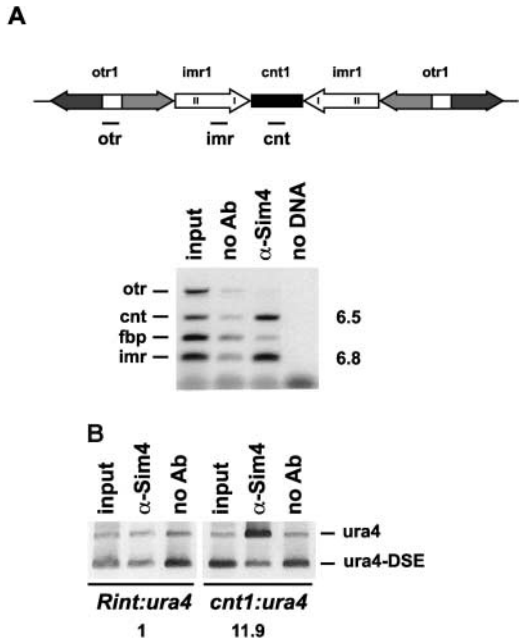

Figure 5. **Sim4 is associated with the centromere central core.** (A) *cnt* and *imr* sequences are enriched in α-Sim4 ChIP. Multiplex PCR analysis. The positions of primers in *cen1* are indicated; *fbp* is a control euchromatic locus. Enrichment of *cnt* and *imr* sequences in ChIPs is compared with the input PCR and expressed relative to *fbp* (right). (B) α-Sim4 ChIP performed on strains (FY4835 and 4837) with *ura4*$^+$ inserted at *Rint* or *cnt1*. PCR with *ura4* primers assays enrichment of *ura4* sequences relative to the *ura4-DSE* minigene at the endogenous locus. Only *ura4* at *cnt1* is enriched in Sim4 ChIPs, indicating that Sim4 can coat noncentromeric DNA inserted at this site. Enrichment of *ura4* in the α-Sim4 ChIPs relative to the input is indicated.

that noncentromeric DNA inserted into the central core can be incorporated into structures closely associated with Sim4.

Sim4 coimmunoprecipitates with the central core kinetochore component, Mis6

The fission yeast kinetochore is likely to be a massive multiprotein complex made up of smaller subcomplexes. To investigate protein–protein interactions at the fission yeast kinetochore, we asked whether Sim4 coimmunoprecipitates with other kinetochore components. Immunoprecipitation with α-HA, α-GFP, or α-Sim4 antibodies was performed on extracts from a strain containing Mis6–HA and Sim4–GFP. Immunoprecipitates (IPs) were analyzed by Western blotting with complementary antibodies. Mis6–HA and Sim4–GFP clearly coimmunoprecipitated (Fig. 6 A). This complex appeared to be very tightly associated, as washing IPs with high concentrations of salt, urea, or nonionic detergents failed to disrupt it (unpublished data). This complex is specific, as Sim4 does not coimmunoprecipitate with other kinetochore proteins, such as Mis12 (unpublished data; Goshima et al., 1999).

Mis6 is required for kinetochore localization of Sim4

Because Mis6 and Sim4 exist in a kinetochore subcomplex, we investigated whether they are required for each other's localization at the centromere. Centromere localization of Sim4 was greatly reduced at the permissive temperature (25°C) and abolished at the restrictive temperature (36°C) in a *mis6* mutant (Fig. 6 B). To quantify this effect, ChIP experiments were performed (Fig. 7 A). At 36°C, there was a large reduction in Sim4 associated with *cnt* and *imr* sequences in the *mis6* mutant compared with wild type (approximately fivefold reduction, within the limits of the multiplex PCR quantification method). Western blotting

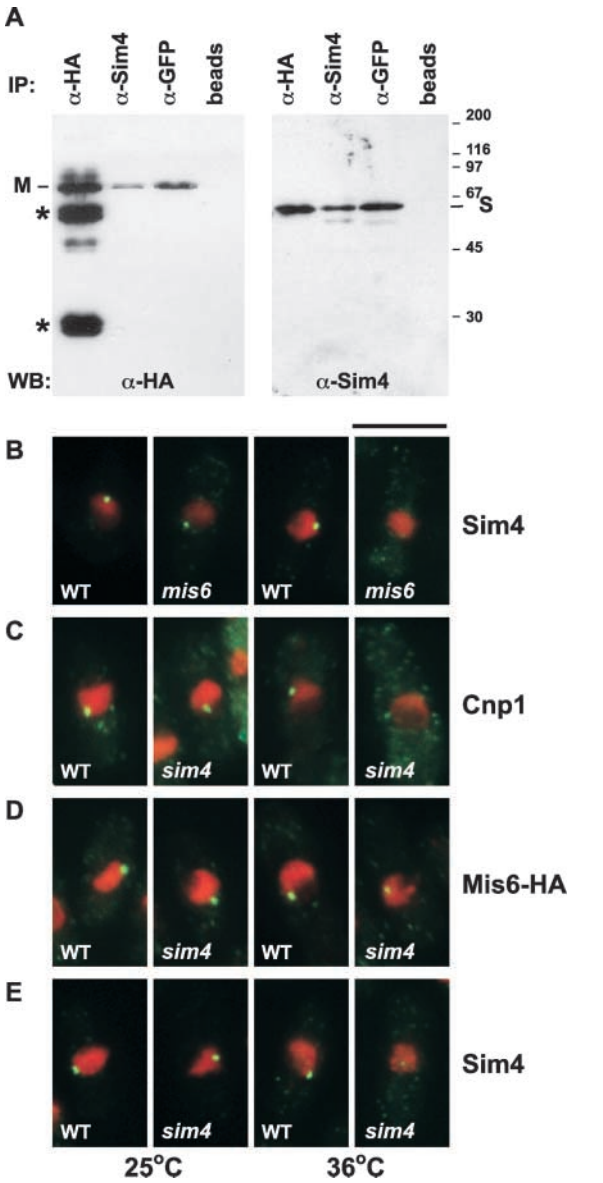

Figure 6. **Sim4–Mis6 complex and kinetochore dependency relationships.** (A) Extracts were prepared from cells expressing Mis6–HA and Sim4–GFP (FY5237). IPs were performed with the indicated antibodies, or beads only as a negative control. IPs were analyzed on Western blots with either α-HA or α-Sim4 antibodies. The positions of Mis6–HA (M), Sim4–GFP (S), IgG (asterisk), and standards are shown. (B–E) Strains (FY3027, 5691, 4536, 5903, and 5900) were grown at 25°C or shifted to 36°C for 6 h before fixation and processing for immunolocalization with the antibodies (green) indicated at right, and DAPI staining (red). Bar, 5 μm. (B) Sim4 localization in wild type and *mis6* mutant. (C) Cnp1 localization in wild type and *sim4* mutant. (D) Mis6–HA localization in wild type and *sim4* mutant. (E) Sim4 localization in wild type and *sim4* mutant.

The Journal of Cell Biology

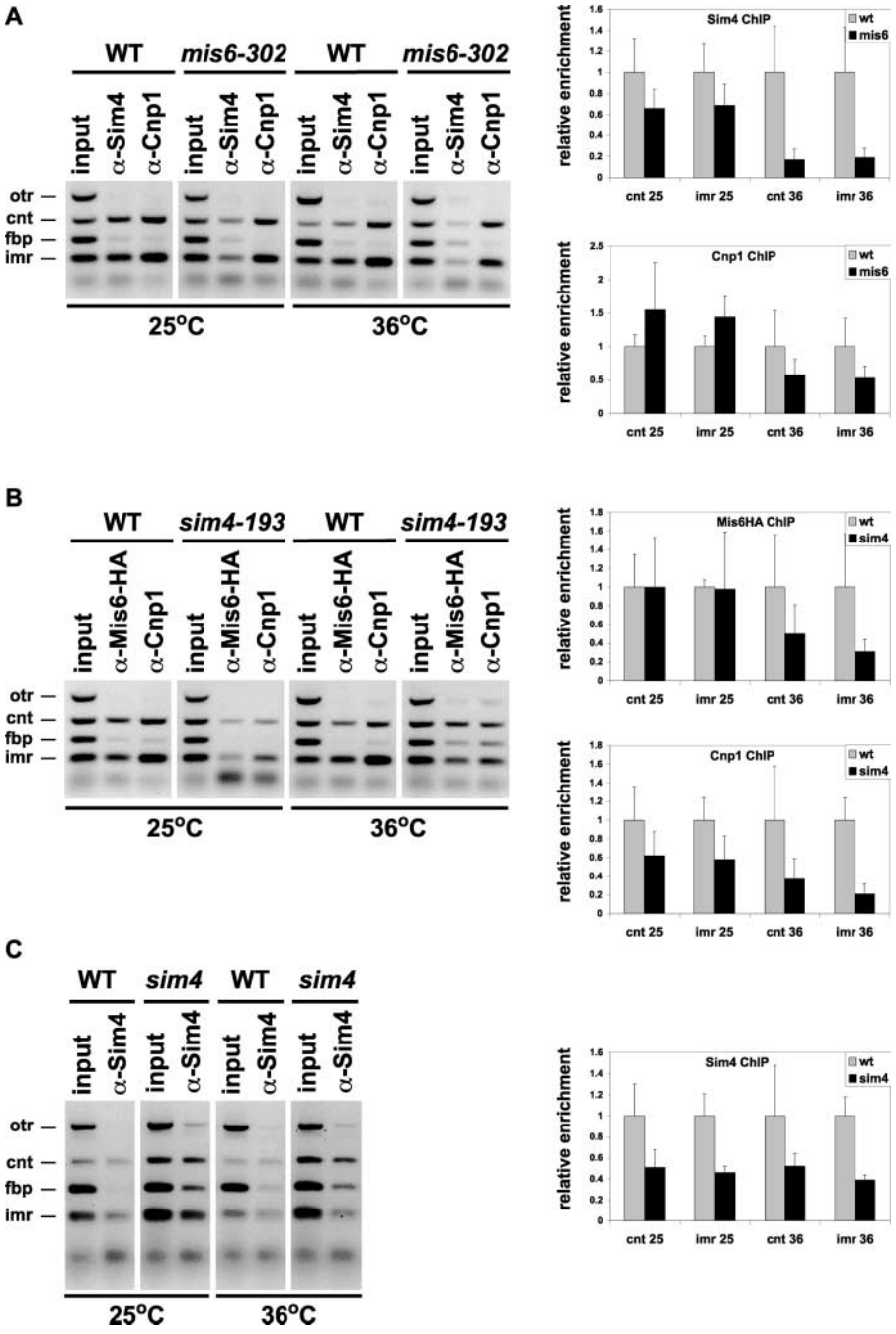

Figure 7. **ChIP analysis of dependency relationships for kinetochore localization.** Strains (FY3027, 5691, 4536, 5903, and 5900) were grown at 25°C or shifted to 36°C for 6 h for ChIP with the indicated antibodies. Left, multiplex PCR analysis of ChIPs. Right, quantification of ChIP PCR data. *cnt* and *imr* enrichment is measured relative to the *fbp* euchromatic control and normalized to the input PCR. For each site/temperature, the mutant value has been normalized to the wild-type value. Data in A and B are from four to six separate ChIP measurements, and data in C are from three separate ChIPs. (A) Sim4 and Cnp1 ChIP in wild type and *mis6* mutant at 25°C and 36°C. (B) Mis6–HA and Cnp1 in wild type and *sim4* mutant at 25°C and 36°C. (C) Sim4 ChIP in wild type and *sim4* mutant at 25°C and 36°C. The PCR of wild-type input at 36°C and, to a lesser extent, at 25°C shows bias of extracted chromatin (little *cnt* and *imr* chromatin). The ChIP PCR is compared with this input, and therefore, there is a relative enrichment of *cnt* and *imr* sequences.

confirmed that there were similar amounts of Sim4 protein in wild-type and *mis6* cells (unpublished data). As Mis6 has been proposed to function as a loading factor for Cnp1 in fission yeast, we also performed Cnp1 ChIP, using antiserum raised to a Cnp1 NH_2-terminal peptide (amino acids 1–19). A decrease in the amount of endogenous Cnp1 associated with *cnt* and *imr* was observed in the *mis6* mutant incubated at 36°C (Fig. 7 A), consistent with results obtained with HA-tagged Cnp1 (Takahashi et al., 2000).

Cnp1 localization was investigated in a *sim4* mutant; a reduction in localization was apparent cytologically (Fig. 6 C) and by ChIP (Fig. 7 B). Cnp1 association with central domain sequences was reduced at 36°C in the *sim4* mutant compared with wild type. Association of Mis6–HA with the central domain was reduced in the *sim4* mutant (Fig. 6 D; Fig. 7 B). The mutant Sim4 protein, itself, showed reduced centromere association (Fig. 6 E; Fig. 7 C). These observations indicate that functional Mis6 is required for localization of Sim4 to the centromere central domain, and that Sim4 is required for localization of wild-type levels of Cnp1 and Mis6.

Genetic interactions between *sim* mutants

Genetic interactions were investigated between *sim* mutants and mutants in other known kinetochore proteins. Overexpression of Sim2/Cnp1^{CENP-A} suppressed the temperature sensitivity of the other *sim* mutants to varying extents (Table I). Overexpression of Sim4 suppressed *mis6* and *sim3*, but

The Journal of Cell Biology

Table I. **High-copy suppression of *sim* mutants**

	Sim1	Cnp1	Sim4	Mis6
sim1-106	**++++**	+++	−	+(+)
sim2-76	−	**++++**	−	ND
sim3-143	++	+++	+++	−
sim4-193	++	+	**++++**	−
mis6-302	+	+	+++(+)	**++++**

Mutants containing multicopy genomic plasmids bearing the indicated gene were assayed by serial dilution on −leu plates at temperatures 25–36°C. Growth was compared to mutant with empty plasmids (equivalent to "−") and to growth with bona fide ORF for each mutant (**++++**, bold).

Table II. **Synthetic interactions of *sim* mutants**

	sim1	*sim2*	*sim3*	*sim4*	*mis6*
sim1					
sim2	SL				
sim3	SL	SL			
sim4	SL	SL	SL		
mis6	S--[a]	+	+	+	
mis12	S--	S--	S---	S--	ND
mal2	S---	S---	SL/S---	S---	ND
nda3	S---	S-	S-	S---	ND
rik1	S-	+	+	+/S-	+/S-
bub1	S---	+	S---	+	+
bub3	+	+	S--	+	ND
mad2	+	+	ND	S--	+
mad3	+	+	+	+	ND

SL, synthetically lethal; +, no growth impairment compared with single mutants; S-, S--, S---, synthetic interaction, degree of growth impairment compared with single mutants.
[a]*sim1mis6* double mutants initially grew very poorly after germination of spores after tetrad dissection, but subsequent growth was only slightly impaired compared with single mutants.

not *sim1* or *sim2*. A genomic clone bearing the putative *sim1*$^+$ ORF (unpublished data) also partially suppressed *sim3* and *sim4* and slightly suppressed *mis6*, but not *sim2*. Overexpression of Mis6 partially suppressed *sim1*, but not *sim3* or *sim4*. In all cases tested, the bona fide *sim*$^+$ gene complemented the temperature sensitivity and reimposed silencing at *cnt1*:*arg3*, whereas multicopy extragenic suppressors allowed only improved growth at the restrictive temperature but did not reimpose central core silencing (unpublished data).

All double mutant combinations between two *sim* mutants were synthetically lethal (Table II). *sim1* was the only mutant with which *mis6* or *mis12* showed any synthetic phenotype (Table II; unpublished data). All *mal2sim*$^-$ double mutants were severely growth impaired compared with the single mutants. *sim1* and *sim4* showed a slight synthetic interaction with *rik1Δ*. Double mutants between *sim* mutants and the α-tubulin mutant *nda3* showed growth impairment, particularly for *sim1* and *sim4*. Surprisingly, there was no synthetic lethality observed between *sim* mutants, or *mis6*, and the spindle checkpoint mutants *bub1*, *bub3*, *mad2*, and *mad3*. Exceptions to this pattern were the *sim1bub1* and *sim3bub1* double mutants, which were highly growth impaired.

These genetic interactions are indicative of functional interactions between Sim proteins and other kinetochore components. They also suggest that Sim proteins yet to be identified, such as Sim3, are likely to function at the kinetochore.

Discussion

We have exploited transcriptional silencing at the fission yeast centromere to facilitate the direct identification of mutants that affect centromere–kinetochore function. The advantage of this screen over those based on minichromosome transmission is that it leads immediately to the identification of mutants that affect kinetochore function, rather than a variety of factors important for chromosome maintenance, such as DNA replication and spindle function. Alleviation of silencing screens have not been used in other organisms for the identification of kinetochore components. The fact that *sim2*$^+$ encodes Cnp1$^{CENP\text{-}A}$ and Sim4 is a novel kinetochore protein specifically associated with the centromere central core region validates this approach. This screen could lead to the identification of chromatin assembly factors that promote the deposition of Cnp1$^{CENP\text{-}A}$. Factors that regulate centromere–kinetochore function, for instance, chromatin-modifying enzymes such as deacetylases and methylases that would transiently associate with the centromere or modify components before centromere association, might also have a *sim* phenotype. The *sim* screen is likely to be very fruitful, as it has already identified two kinetochore components. In addition, the Sim1 protein is centromere associated (Abbott, J., personal communication; unpublished data). There are at least three more *sim* complementation groups (unpublished data). It is also clear that the *sim* screen is not saturated; whereas 11 alleles of *sim1* were isolated, only one allele of *sim4* was recovered. *mis6* and *mal2* mutants, known to alleviate central core silencing, were not recovered. It is not yet known what distance from centromeric DNA kinetochore components can be in order to alleviate centromere silencing when defective. However, the *sim* screen is unlikely to identify components, such as Dis1, that only transiently associate with kinetochores during mitosis (Nakaseko et al., 2001).

Our characterization of Sim4 shows that it colocalizes with Mis6 and is restricted to the central domain of fission yeast centromeres. The *sim4* mutant exhibits altered central core chromatin structure, elevated rates of chromosome loss, and increased sensitivity to MT poisons. Mitosis is frequently aberrant, with lagging chromosomes and nondisjunction of sister chromatids. These phenotypes indicate that Sim4 is required for kinetochore function. Given that neocentromere formation in other organisms requires the association of kinetochore components with noncentromeric DNA, it is of interest that Sim4 is capable of coating a *ura4*$^+$ gene inserted in the central core.

Sim4 displays many functional interactions with the kinetochore protein Mis6; Sim4 and Mis6 are in the same complex, and overexpression of Sim4 strongly suppresses *mis6*. Association of Sim4 with the centromere is strongly dependent on Mis6, and the converse is true to a lesser degree. Sim4 is a small coiled-coil protein; many such proteins exist in kinetochore complexes in budding yeast (Cheeseman et al., 2002). Although no definite Sim4 homologues can be

The Journal of Cell Biology

The Journal of Cell Biology

identified in metazoa or other organisms, we have noticed a weak similarity in structure and sequence between Sim4 and vertebrate CENP-H (25% similarity; Fig. S2; Sugata et al., 1999, 2000; Fukagawa et al., 2001). In chicken DT40 cells, the Mis6 homologue, CENP-I, is required for kinetochore localization of CENP-H (Nishihashi et al., 2002), as Mis6 is required for Sim4 localization. A two-hybrid interaction between CENP-H and CENP-I has also been reported (Nishihashi et al., 2002), suggesting that they are part of a complex. The observed similarities in behavior between *S. pombe* Sim4 and chicken CENP-H add weight to the weak homology between the two.

A *mis6* mutant is defective in centromere incorporation of newly synthesized GFP-tagged Cnp1 (expressed from a heterologous promoter) at the restrictive temperature, and there is a reduced level of Cnp1^{CENP-A}–HA (expressed from its endogenous promoter). These observations have led to the proposal that Mis6 acts as a loading factor for Cnp1^{CENP-A} (Takahashi et al., 2000). We have observed that both *mis6* and *sim4* mutants display reduced association of Cnp1 with the centromere, and this could be interpreted as evidence for a Mis6/Sim4-containing complex that acts as a specific loading factor for Cnp1. However, the budding yeast Mis6 homologue, Ctf3p, is not required for loading of Cse4p (Measday et al., 2002), the CENP-A counterpart. In addition, chicken CENP-I/Mis6 is not required for the localization of CENP-A, but, like CENP-H, it is required for CENP-C localization (Fukagawa et al., 2001; Nishihashi et al., 2002). These inconsistencies may reflect differences in organization and details between different organisms. However, several central core mutants affect Cnp1^{CENP-A} centromere association, including *sim1*, *sim3*, and *sim7* (Abbott, J., personal communication; unpublished data) as well as *sim4* and *mis6*. We favor the idea that although specific loading or assembly factors for Cnp1 probably exist, it is the presence of a fully functional kinetochore that directs the incorporation of newly synthesized Cnp1^{CENP-A} into the centromere, cell cycle after cell cycle. One possibility is that Cnp1^{CENP-A} is only correctly incorporated at mitosis when proper kinetochore–MT attachments produce tension at functional kinetochores (Mellone and Allshire, 2003). Such a model is attractive, as it could play a part in the epigenetic inheritance of centromere site and specification.

Similar to other mutants that affect central domain function, *sim4* mutants disrupt its unique chromatin structure (Saitoh et al., 1997; Goshima et al., 1999; Takahashi et al., 2000; Jin et al., 2002). Cnp1 is present at high levels in the central core and may take the place of histone H3 in the nucleosomes of this region. *mis6* and *sim4* mutants, amongst others, have reduced Cnp1^{CENP-A} in the central domain. The smear pattern suggests that central core chromatin is organized in such a way that accessibility to MNase is altered; DNA may be wrapped more loosely around Cnp1-containing nucleosomes. Alternatively, the nucleosomes in this region may not have a regular spacing of ~150 bp, but may be nonregularly spaced. Perhaps the fully assembled kinetochore protects the central core chromatin, not only from transcription factors, but also from activities that induce regular nucleosomal spacing or loading of histone H3. Whatever the cause of the unusual chromatin, it correlates with transcriptional silencing, normal levels of Cnp1^{CENP-A}, and kinetochore integrity.

Mutants that alleviate outer repeat silencing have high levels of lagging chromosomes and are supersensitive to MT-disrupting drugs (Ekwall et al., 1996, 1999), indicative of defects in MT interaction or in the coordination of MT-binding sites on single kinetochores. It is likely that lagging chromosomes are due to merotelic attachment of kinetochores, in which a single kinetochore interacts with MTs emanating from both spindle poles (Ladrach and LaFountain, 1986; Pidoux et al., 2000; Yu and Dawe, 2000; Stear and Roth, 2002). The Swi6-containing heterochromatin of the outer repeats that is required for centromeric cohesion may also have a role in preventing merotelic attachment (Pidoux et al., 2000; Bernard et al., 2001; Nonaka et al., 2002). Merotelic attachment has been shown to be a major mechanism contributing to aneuploidy in mammalian tissue culture cells (Cimini et al., 2001, 2002). Mutants that alleviate central core silencing or proteins that are located at the central core fall into two classes. Mutants of the first class, e.g., *mis6* and *cnp1*/*sim2*, display uneven chromosome segregation, with few lagging chromosomes. It has been proposed that Mis6 is required for the biorientation function of the kinetochore, ensuring that the sister kinetochores face in opposite directions (Saitoh et al., 1997); *mis6* mutants would not have a defect in kinetochore–MT interaction, per se, which is consistent with their observed wild-type sensitivity to MT drugs. A second class of central core mutants is typified by *sim1*, *sim3*, and *sim4*. These display both uneven segregation and lagging chromosomes and are sensitive to MT drugs. *sim1* and *4* also display stronger synthetic interactions with the α-tubulin mutant *nda3* than does *cnp1*/*sim2*. We propose that Sim4, and other members of this class, is required both for the biorientation of sister kinetochores and for assembling a fully functional kinetochore in which the multiple MT-binding sites are locked together so that they interact correctly with the mitotic spindle. Although Mis6 and Sim4 are in the same complex, and may cooperate functionally, genetic evidence suggests that their functions overlap but are not identical; *sim4* is synthetically lethal with *sim1*, *sim2*/*cnp1*, and *sim3*, but *mis6* is not. The fact that overexpression of Sim4 suppresses *mis6*, but not vice versa, suggests that Sim4 acts upstream of Mis6. The lack of interaction with checkpoint components suggests that the spindle checkpoint may be impaired in *sim* mutants; the fact that these mutants do not exhibit a strong arrest at metaphase is consistent with this. Analyses of Bub1 have suggested that it may play additional roles at kinetochores independent of its role in checkpoint function (Warren et al., 2002).

We have used centromeric silencing in fission yeast as an assay of kinetochore assembly and successfully identified Cnp1^{CENP-A} and a novel kinetochore component, Sim4. This is clearly a very effective approach for the identification of additional kinetochore components. By investigating genetic interactions in conjunction with protein–protein interactions and dependency relationships for localization, we aim to build up a detailed picture of the architecture and function of this complex kinetochore.

Table III. **List of strains used in this study**

Strain	Genotype
972	*h⁻*
1645	*h⁺ ade6-210 arg3-D4 his3-D1 leu1-32 ura4-D18*
1646	*h⁻ ade6-210 arg3-D4 his3-D1 leu1-32 ura4-D18*
1647	*h⁺ ade6-216 arg3-D4 his3-D1 leu1-32 ura4-D18*
1648	*h⁻ ade6-216 arg3-D4 his3-D1 leu1-32 ura4-D18*
1891	*h⁻ cnt1*(NcoI):*ura4 ade6-210 arg3-D4 his3-D1 leu1-32 ura4-D18*
2221	*h⁻ cnt1*(NcoI):*arg3 ade6-210 leu1-32 ura4-D18 arg3-D4 his3-D1*
944	*h⁻ otr2*(HindIII):*ura4 ade6-210 leu1-32 ura4-DSE*
1895	*h⁻ rik1::LEU2 cnt3:ura4 ade6-210 arg3-D4 his3-D1 leu1-32 ura4-D18/-DSE*
382	*h⁺ cnt3*(NcoI):*ade6 ade6-DNN leu1-32 ura4-D18*
1869	*h⁹⁰ otr1R*(SphI):*ade6 tel1*L:*his3 ade6-210 his3-D1 leu1-32 ura4-DSE*
3027	*h⁺ cnt1*(NcoI):*arg3 cnt3*(NcoI):*ade6 otr2*(HindIII):*ura4 tel1*L:*his3 ade6-210 leu1-32 ura4-D18 arg3-D4 his3-D1*
3033	*h⁻ cnt1*(NcoI):*arg3 cnt3*(NcoI):*ade6 otr2*(HindIII):*ura4 tel1*L:*his3 ade6-210 leu1-32 ura4-D18 arg3-D4 his3-D1*
4484	*h⁺ sim1-106 cnt1:arg3 cnt3:ade6 otr2:ura4 tel1*L:*his3 ade6-210 leu1-32 ura4-D18 arg3-D4 his3-D1*
4485	*h⁻ sim1-106 cnt1:arg3 cnt3:ade6 otr2:ura4 tel1*L:*his3 ade6-210 leu1-32 ura4-D18 arg3-D4 his3-D1*
4461	*h⁺ sim2-76 cnt1:arg3 cnt3:ade6 otr2:ura4 tel1*L:*his3 ade6-210 leu1-32 ura4-D18 arg3-D4 his3-D1*
4462	*h⁻ sim2-76 cnt1:arg3 cnt3:ade6 otr2:ura4 tel1*L:*his3 ade6-210 leu1-32 ura4-D18 arg3-D4 his3-D1*
4504	*h⁺ sim3-143 cnt1:arg3 cnt3:ade6 otr2:ura4 tel1*L:*his3 ade6-210 leu1-32 ura4-D18 arg3-D4 his3-D1*
4502	*h⁻ sim3-143 cnt1:arg3 cnt3:ade6 otr2:ura4 tel1*L:*his3 ade6-210 leu1-32 ura4-D18 arg3-D4 his3-D1*
4536	*h⁺ sim4-193 cnt1:arg3 cnt3:ade6 otr2:ura4 tel1*L:*his3 ade6-210 leu1-32 ura4-D18 arg3-D4 his3-D1*
4540	*h⁻ sim4-193 cnt1:arg3 cnt3:ade6 otr2:ura4 tel1*L:*his3 ade6-210 leu1-32 ura4-D18 arg3-D4 his3-D1*
5691	*h mis6-302 cnt1:arg3 cnt3:ade6 otr2:ura4 tel1*L:*his3 ade6-210 leu1-32 ura4-D18 arg3-D4 his3-D1*
3606	*h^A rik1::LEU2+ cnt1:arg3 cnt3:ade6 otr2:ura4 tel1*L:*his3 ade6-210 leu1-32 ura4-D18 arg3-D4 his3-D1*
4575	*h mal2-1 cnt1:arg3 cnt3:ade6 otr2:ura4 tel1*L:*his3 ade6-210 leu1-32 ura4-D18 arg3-D4 his3-D1*
4835	*h⁻ Rint:ura4 ura4-DSE leu1-32 his3-D1 arg3-D4*
4837	*h⁻ cnt1*(NcoI):*ura4 ura4-DSE leu1-32 his3-D1 arg3-D4*
4841	*h⁻ otr1R*(SphI):*ura4 ura4-DSE leu1-32 his3-D1 arg3-D4*
5711	*h sim1-106 Rint:ura4 ura4-DSE**
5717	*h sim1-106 cnt1*(NcoI):*ura4 ura4-DSE**
5674	*h sim1-106 otr1R*(SphI):*ura4 ura4-DSE**
5695	*h sim3-143 Rint:ura4 ura4-DSE**
5719	*h sim3-143 cnt1*(NcoI):*ura4 ura4-DSE**
5683	*h sim3-143 otr1R*(SphI):*ura4 ura4-DSE**
5714	*h sim4-193 Rint:ura4 ura4-DSE**
5720	*h sim4-193 cnt1*(NcoI):*ura4 ura4-DSE**
5688	*h sim4-193 otr1R*(SphI):*ura4 ura4-DSE**
4636	*h⁻ cut9-665 leu1-32 ura4-DSE ade6-210 his1-102*
5254	*h⁻ sim4-193 cut9-665**
3990	*h⁺ cnt1:arg3 otr2:ura4 tel1:his3 [Ch16 ade6-216 LEU2⁺] ade6-210 ura4-D18 leu1-32 his3-D1 arg3-D4*
4005	*h sim1-106 cnt1:arg3 otr2:ura4 tel1:his3 [Ch16 ade6-216 LEU2⁺] ade6-210 ura4-D18 leu1-32 his3-D1 arg3-D4*
4015	*h sim2-76 cnt1:arg3 otr2:ura4 tel1:his3 [Ch16 ade6-216 LEU2⁺] ade6-210 ura4-D18 leu1-32 his3-D1 arg3-D4*
4022	*h sim3-143 cnt1:arg3 otr2:ura4 tel1:his3 [Ch16 ade6-216 LEU2⁺] ade6-210 ura4-D18 leu1-32 his3-D1 arg3-D4*
4025	*h sim4-193 cnt1:arg3 otr2:ura4 tel1:his3 [Ch16 ade6-216 LEU2⁺] ade6-210 ura4-D18 leu1-32 his3-D1 arg3-D4*
1317	*h⁺ swi6::his1⁺ ade6-210 his1-102 leu1-32 ura4-DSE [Ch16 ade6-216 LEU2⁺]*
5077	*h⁻ sim4::sim4GFP-kanMX6 cnt1:arg3 cnt3:ade6 otr2:ura4 tel1*L:*his3 ade6-210 leu1-32 ura4-D18 arg3-D4 his3-D1*
5251	*h⁻ sim4::sim4GFP-kanMX6 ade6-210 leu1-32 ura4-D18 arg3-D4 his3-D1*
5237	*h⁻ sim4::sim4-GFP-kanMX6 mis6::mis6-3HA-LEU2⁺ ade6-210 leu1-32 ura4-D18 his3-D1 cnt1:arg3 or arg3⁺*
2919	*h⁻ mis6-302 leu1-32*
3119	*h⁻ mis6-302 cnt1:ura4 ura4-DSE leu1-32**
3272	*h mis6-302 cnt1:ura4 ura4-DSE leu1-32**
2929	*h⁻ mis6::mis6-3HA-LEU2⁺ RInt:ura4 ura4-DSE ade6-210 leu1-32*
2930	*h⁺ mis6::mis6-3HA-LEU2⁺ cnt1:ura4 ura4-DSE ade6-210 leu1-32*
5895	*h⁺ sim4-193 mis6::mis6-3HA-LEU2⁺ RInt:ura4 ura4-DSE leu1-32**
5900	*h⁻ sim4-193 mis6::mis6-3HA-LEU2⁺ cnt1:ura4 ura4-DSE leu1-32**
5903	*h⁻ mis6::mis6-3HA-LEU2⁺ cnt1:ura4 ura4-DSE leu1-32**
5958	*h/h⁺ sim4⁺/sim4::sim4GFP-kanMX6 ade6-210/ade6-216 leu1-32/leu1-32 ura4-D18/ura4-D18 arg3-D4/arg3-D4 his3-D1/his3-D1*
5959	*h/h⁺ sim4⁺/sim4::ura4 ade6-210/ade6-216 leu1-32/leu1-32 ura4-D18/ura4-D18 arg3-D4/arg3-D4 his3-D1/his3-D1*
845	*h⁻ nda3-km311 leu1-32*
3828	*h⁻ mis12-537 leu1-32*

Genotypes of strains used. For strains marked with an asterisk (*), only the relevant genotype is listed.

The Journal of Cell Biology

The Journal of Cell Biology

Materials and methods

Standard techniques

Chemicals were obtained from Sigma-Aldrich unless stated otherwise. Standard procedures were used for bacterial and fission yeast growth, genetics, and manipulations (Moreno et al., 1991).

Yeast strains

S. pombe strains used in this study are shown in Table III. To insert the promoter-crippled *arg3*$^+$ gene at *cnt1*, an *arg3*$^+$ fragment with 181 bp upstream of the ATG, including the TATA box but lacking other promoter elements, was PCR amplified and cloned into NcoI-digested pKS-cnt1, which contains a 5.2-kb EcoRI *cnt1* fragment (Fig. 1 A). The *cnt1*(NcoI)*:arg3*$^+$ fragment was transformed into strain FY1891 (Allshire et al., 1994). An FOA-resistant, arg+ colony was analyzed by Southern blotting. Crosses with strains FY944, 1895, 382, and 1869 created strains FY3027 and 3033.

Screen for mutants that alleviate central core silencing

FY3027 or 3033 cells were spread on −arg PMG plates, irradiated with 3–5 mJ UV (50–80% killing), and incubated at 25°C for 5–20 d, and fast-growing colonies were picked from the background of slower-growing colonies. Reproducibly fast growers on −arg were tested for thermo- and cryosensitivity, for supersensitivity to TBZ, and for maintenance of silencing at *otr2:ura4* and *tel1L:his3*. Mutants were backcrossed at least three times and placed in complementation groups. *sim2*$^+$ and *sim4*$^+$ genes were identified by complementation of the temperature-sensitive phenotype with a genomic library (pDB).

Analysis of genetic interactions

Synthetic lethality. At least 30 asci were dissected on YES plates and incubated at 25°C. The growth of viable double mutants compared with single mutants was assessed on YES phloxine B at 25°C, 28°C, 30°C, 32°C, 34°C, and 36°C.

Multicopy suppression. *sim* mutants were transformed with genomic plasmids (pDB) bearing *sim4*$^+$, *cnp1*$^+$/*sim2*$^+$, and *sim1*$^+$ ORFs. A genomic fragment bearing the *mis6*$^+$ ORF was PCR amplified and cloned into pAL-KS. Growth of serial dilutions was assessed on PMG phloxine B and PMG −arg and compared with the relevant empty plasmid.

Micrococcal nuclease digestion of chromatin

MNase digestion of chromatin in permeabilized cells was performed as previously described (Allshire et al., 1994), except that cells were grown in YES and spheroplasted with zymolyase-100T (ICN Biomedicals).

RT-PCR

Total RNA was prepared from strains grown in YES at 25°C or shifted to 36°C for 6 h, and RT-PCR was performed as previously described (Ekwall et al., 1997). The *ura4* and *ura4-DSE* PCR products were separated on 1.5% agarose gels and poststained with ethidium bromide or SYBR green (Molecular Probes) according to the manufacturer's instructions. Quantitation of bands was performed using the Eastman Kodak Co. EDAS 290 system and 1D Image Analysis software. Analysis was performed two to four times at each temperature, and average values from these experiments are presented (Fig. 1 E). The *ura4* to *ura4-DSE* ratio was determined and expressed relative to wild type at 25°C for each site, *Rint*, *cnt1*, or *otr1*.

Production of antibodies, Western blotting, and immunoprecipitations

sim4$^+$ cDNA was PCR amplified and cloned into pGEX-4T1 (Amersham Biosciences). GST–Sim4 fusion protein was purified and used to immunize a sheep. α-Sim4 antibodies were affinity purified on nitrocellulose. Antibodies for Western blotting were diluted in PBS-Tween as follows: α-Sim4, 1:300; α-HA, 1:300; α-GFP, 1:2,000 (in 1% milk; Molecular Probes). Blots were developed using ECL reagents (Amersham Biosciences). Immunoprecipitations were performed as previously described (Millband and Hardwick, 2002).

ChIP

ChIP was performed as previously described (Ekwall and Partridge, 1999; Jin et al., 2002), except for the following modifications. For growth at restrictive temperature, cells were shifted to 36°C for 6 h. After addition of formaldehyde, incubation was continued at 36°C for 5 min, followed by 3 min in an ice-water bath and 22 min at 18°C (cells grown at 25°C were fixed for 30 min at 18°C). Cells were spheroplasted at 10^8 cells/ml in PEMS (100 mM Pipes, pH 7, 1 mM EDTA, 1 mM $MgCl_2$, 1.2 sorbitol) + 0.4 mg/ml zymolyase-100T for 25 min at 36°C. Cells were washed twice in PEMS, and cell pellets were frozen at −20°C. Thereafter the standard ChIP procedure was followed (Ekwall and Partridge, 1999). 10 μl α-Cnp1 antiserum (Kniola et al., 2001), 30 μl affinity-purified α-Sim4 antibody, or 30 μl α-HA antibody was used in ChIPs. Multiplex PCR analysis was performed as previously described (Jin et al., 2002). PCR products were quantified as described for RT-PCR. For the input PCR, the *cnt*, *imr*, and *otr* values were normalized to the *fbp* value, giving the input ratio. Enrichment of *cnt*, *imr*, and *otr* bands in the ChIPs was calculated relative to the *fbp* band and then corrected for the ratio obtained in the input PCR. Steps were taken to check that the multiplex PCR was a good method for quantification of ChIPs. The quantification depends on a quantifiable *fbp* band being present and if necessary exposure times, or amount of template, were adjusted to ensure that this was the case. PCR performed on different dilutions of input and ChIP'd samples gave very similar results. Although there was variation in the actual values obtained between individual ChIP experiments (producing the error bars in Fig. 7), the fold reductions seen in mutants were consistent between experiments. ChIP performed on strains with *ura4*$^+$ insertions at *Rint* or *cnt1* was analyzed by PCR as previously described (Ekwall et al., 1997).

Cytology

Immunofluorescence was performed as previously described (Pidoux et al., 2000), except that cells were fixed for 5–10 min in 3.7% freshly prepared formaldehyde for staining with α-Sim4 antibodies. For immunolabeling of MTs, cells were fixed for 10–15 min in 3.7% formaldehyde, 0.05% glutaraldehyde. The following antibodies were used: sheep α-Cnp1 antiserum (1:300), mouse 12CA5 α-HA (1:30), mouse TAT1 α-tubulin (1:15), and affinity-purified sheep α-Sim4 antibody (1:30). FITC (Sigma-Aldrich), Texas red (Jackson ImmunoResearch Laboratories), or Alexa®488 (Molecular Probes)-conjugated secondary antibodies were used at 1:100 or 1:1,000. FISH was performed as previously described (Ekwall et al., 1996). Microscopy was performed as previously described (Pidoux et al., 2000) or using the following setup: 100× Plan Neofluar 1.3 NA objective on a Carl Zeiss MicroImaging, Inc. Axioplan 2 IE fluorescence microscope equipped with Chroma 83000 and 86000 filter sets, Prior ProScan filterwheel (Prior Scientific), and Photometrics CoolSnapHQ CCD camera (Roper Scientific). Image acquisition was controlled using Metamorph software (Universal Imaging Corp.).

For measurement of spindle lengths, *cut9* and *cut9sim4* strains were grown at 25°C and shifted to 36°C for 4 h. Alternatively, wild-type and *sim4* cells containing pREP3X-*mad2* (He et al., 1997) were grown at 25°C in the absence of thiamine for 16 h, and then cells were shifted to 36°C for 7 h in the same medium. Spindle length was measured in cells with unseparated chromosomes, where both spindle poles were in focus, using either IPLab or Metamorph software. Spindle length was measured in 100–300 cells for each strain.

Online supplemental material

The supplemental figures (Figs. S1 and S2) for this article are available at http://www.jcb.org/cgi/content/full/jcb.200212110/DC1. These figures include minichromosome loss data, *sim4*$^+$ sequence and alignment with HsCENP-H, as well as Western blotting data and description of the *sim4*$^+$ knockout.

We are very grateful to W. Earnshaw, U. Fleig, I. Hagan, K. Hardwick, K. Gull, B. Mellone, T. Nakamura, S. Sazer, and M. Yanagida for strains, antibodies, and reagents. We thank Paul Perry for microscopy support, J. Abbott, K. Hardwick, B. Earnshaw, and B. Mellone for critical reading of the manuscript, and past and present members of the Allshire lab for stimulating discussions.

This research was supported by a Caledonian Research Foundation Fellowship (Royal Society of Edinburgh) to A.L. Pidoux and by the Association for International Cancer Research, the Medical Research Council of Great Britain, and The Wellcome Trust. R.C. Allshire is a Principal Research Fellow of The Wellcome Trust.

Submitted: 18 December 2002
Revised: 5 March 2003
Accepted: 7 March 2003

References

Allshire, R.C., J.-P. Javerzat, N.J. Redhead, and G. Cranston. 1994. Position effect variegation at fission yeast centromeres. *Cell.* 76:157–169.

Allshire, R.C., E.R. Nimmo, K. Ekwall, J.-P. Javerzat, and G. Cranston. 1995. Mutations derepressing silent centromeric domains in fission yeast disrupt chromosome segregation. *Genes Dev.* 9:218–233.

Bahler, J., J.Q. Wu, M.S. Longtine, N.G. Shah, A. McKenzie, A.B. Steever, A. Wach, P. Philippsen, and J.R. Pringle, Jr. 1998. Heterologous modules for efficient and versatile PCR-based gene targeting in *Schizosaccharomyces pombe. Yeast.* 14:943–951.

Bannister, A.J., P. Zegerman, J.F. Partridge, E.A. Miska, J.O. Thomas, R.C. Allshire, and T. Kouzarides. 2001. Selective recognition of methylated lysine 9 on histone H3 by the HP1 chromo domain. *Nature.* 410:120–124.

Bernard, P., J.F. Maure, J.F. Partridge, S. Genier, J.P. Javerzat, and R.C. Allshire. 2001. Requirement of heterochromatin for cohesion at centromeres. *Science.* 294:2539–2542.

Cheeseman, I.M., S. Anderson, M. Jwa, E.M. Green, J. Kang, J.R. Yates, C.S. Chan, D.G. Drubin, and G. Barnes. 2002. Phospho-regulation of kinetochore-microtubule attachments by the Aurora kinase Ipl1p. *Cell.* 111:163–172.

Cimini, D., B. Howell, P. Maddox, A. Khodjakov, F. Degrassi, and E.D. Salmon. 2001. Merotelic kinetochore orientation is a major mechanism of aneuploidy in mitotic mammalian tissue cells. *J. Cell Biol.* 153:517–527.

Cimini, D., D. Fioravanti, E.D. Salmon, and F. Degrassi. 2002. Merotelic kinetochore orientation versus chromosome mono-orientation in the origin of lagging chromosomes in human primary cells. *J. Cell Sci.* 115:507–515.

Ding, R., K.L. McDonald, and J.R. McIntosh. 1993. Three-dimensional reconstruction and analysis of mitotic spindles from the yeast *Schizosaccharomyces pombe. J. Cell Biol.* 120:141–151.

Ekwall, K., and J.F. Partridge. 1999. Fission yeast chromosome analysis. Fluorescence in situ hybridisation (FISH) and chromatin immunoprecipitation (CHIP). *In* Chromosome Structural Analysis: A Practical Approach. W.A. Bickmore, editor. Oxford University Press, Oxford, UK. 38–57.

Ekwall, K., J.-P. Javerzat, K. Lorentz, H. Schmidt, G. Cranston, and R. Allshire. 1995. The chromo domain protein Swi6: A key component at fission yeast centromeres. *Science.* 269:1429–1431.

Ekwall, K., E.R. Nimmo, J.-P. Javerzat, B. Borgström, R. Egel, G. Cranston, and R. Allshire. 1996. Mutations in the fission yeast silencing factors *clr4*$^+$ and *rik1*$^+$ disrupt the localisation of the chromo domain protein Swi6p and impair centromere function. *J. Cell Sci.* 109:2637–2648.

Ekwall, K., T. Olsson, B.M. Turner, G. Cranston, and R.C. Allshire. 1997. Transient inhibition of histone acetylation alters the structural and functional imprint at fission yeast centromeres. *Cell.* 91:1021–1032.

Ekwall, K., G. Cranston, and R.C. Allshire. 1999. Novel fission yeast mutants which alleviate transcriptional silencing in centromeric flanking repeats and disrupt chromosome segregation. *Genetics.* 153:1153–1169.

Fukagawa, T., Y. Mikami, A. Nishihashi, V. Regnier, T. Haraguchi, Y. Hiraoka, N. Sugata, K. Todokoro, W. Brown, and T. Ikemura. 2001. CENP-H, a constitutive centromere component, is required for centromere targeting of CENP-C in vertebrate cells. *EMBO J.* 20:4603–4617.

Goshima, G., S. Saitoh, and M. Yanagida. 1999. Proper metaphase spindle length is determined by centromere proteins Mis12 and Mis6 required for faithful chromosome segregation. *Genes Dev.* 13:1664–1677.

Hahnenberger, K.M., J. Carbon, and L. Clarke. 1991. Identification of DNA regions required for mitotic and meiotic functions within the centromere of *Schizosaccharomyces pombe* chromosome I. *Mol. Cell. Biol.* 11:2206–2215.

He, X., T.E. Patterson, and S. Sazer. 1997. The *Schizosaccharomyces pombe* spindle checkpoint protein Mad2p blocks anaphase and genetically interacts with the anaphase-promoting complex. *Proc. Natl. Acad. Sci. USA.* 94:7965–7970.

He, X., D.R. Rines, C.W. Espelin, and P.K. Sorger. 2001. Molecular analysis of kinetochore-microtubule attachment in budding yeast. *Cell.* 106:195–206.

Garcia, M.A., L. Vardy, N. Koonrugsa, and T. Toda. 2001. Fission yeast ch-TOG/XMAP215 homologue Alp14 connects mitotic spindles with the kinetochore and is a component of the Mad2-dependent spindle checkpoint. *EMBO J.* 20:3389–3401.

Jin, Q.W., A.L. Pidoux, C. Decker, R.C. Allshire, and U. Fleig. 2002. The Mal2p protein is an essential component of the fission yeast centromere. *Mol. Cell. Biol.* 22:7168–7183.

Karpen, G.H., and R.C. Allshire. 1997. The case for epigenetic effects on centromere identity and function. *Trends Genet.* 13:489–496.

Kniola, B., E. O'Toole, J.R. McIntosh, B. Mellone, R. Allshire, S. Mengarelli, K. Hultenby, and K. Ekwall. 2001. The domain structure of centromeres is conserved from fission yeast to humans. *Mol. Biol. Cell.* 12:2767–2775.

Ladrach, K.S., and J.R. LaFountain. 1986. Malorientation and abnormal segregation of chromosomes during recovery from colcemid and nocodazole. *Cell Motil. Cytoskeleton.* 6:419–427.

McIntosh, J.R., E.L. Grishchuk, and R.R. West. 2002. Chromosome-microtubule interactions during mitosis. *Annu. Rev. Cell Dev. Biol.* 18:193–219.

Measday, V., D.W. Hailey, I. Pot, S.A. Givan, K.M. Hyland, G. Cagney, S. Fields, T.N. Davis, and P. Hieter. 2002. Ctf3p, the Mis6 budding yeast homolog, interacts with Mcm22p and Mcm16p at the yeast outer kinetochore. *Genes Dev.* 16:101–113.

Mellone, B.G., and R.C. Allshire. 2003. Stretching it: putting the CEN(P-A) in centromere. *Curr. Opin. Genet. Dev.* 13:191–198.

Millband, D.N., and K.G. Hardwick. 2002. Fission yeast Mad3p is required for Mad2p to inhibit the anaphase-promoting complex and localizes to kinetochores in a Bub1p-, Bub3p-, and Mph1p-dependent manner. *Mol. Cell. Biol.* 22:2728–2742.

Moreno, S., A.J.S. Klar, and P. Nurse. 1991. Molecular genetic analysis of fission yeast *Schizosaccharomyces pombe. Methods Enzymol.* 194:795–823.

Musacchio, A., and K.G. Hardwick. 2002. The spindle checkpoint: structural insights into dynamic signalling. *Nat. Rev. Mol. Cell Biol.* 3:731–741.

Nakaseko, Y., G. Goshima, J. Morishita, and M. Yanagida. 2001. M phase-specific kinetochore proteins in fission yeast: microtubule-associating Dis1 and Mtc1 display rapid separation and segregation during anaphase. *Curr. Biol.* 11:537–549.

Nakayama, J., J.C. Rice, B.D. Strahl, C.D. Allis, and S.I. Grewal. 2001. Role of histone H3 lysine 9 methylation in epigenetic control of heterochromatin assembly. *Science.* 292:110–113.

Nonaka, N., T. Kitajima, S. Yokobayashi, G. Xiao, M. Yamamoto, S.I. Grewal, and Y. Watanabe. 2002. Recruitment of cohesin to heterochromatic regions by Swi6/HP1 in fission yeast. *Nat. Cell Biol.* 4:89–93.

Nasmyth, K. 2002. Segregating sister genomes: the molecular biology of chromosome separation. *Science.* 297:559–565.

Nimmo, E.R., A.L. Pidoux, P.E. Perry, and R.C. Allshire. 1998. Defective meiosis in telomere-silencing mutants of *Schizosaccharomyces pombe. Nature.* 392:825–828.

Nishihashi, A., T. Haraguchi, Y. Hiraoka, T. Ikemura, V. Regnier, H. Dodson, W.C. Earnshaw, and T. Fukagawa. 2002. CENP-I is essential for centromere function in vertebrate cells. *Dev. Cell.* 2:463–476.

Partridge, J.F., B. Borgstrom, and R.C. Allshire. 2000. Distinct protein interaction domains and protein spreading in a complex centromere. *Genes Dev.* 14:783–791.

Partridge, J.F., K.S. Scott, A.J. Bannister, T. Kouzarides, and R.C. Allshire. 2002. Cis-acting DNA from fission yeast centromeres mediates histone H3 methylation and recruitment of silencing factors and cohesin to an ectopic site. *Curr. Biol.* 12:1652–1660.

Pidoux, A.L., and R.C. Allshire. 2000a. Centromeres: getting a grip of chromosomes. *Curr. Opin. Cell Biol.* 12:308–319.

Pidoux, A.L., and R.C. Allshire. 2000b. The structure of yeast centromeres and telomeres and the role of silent heterochromatin. *In* The Yeast Nucleus. J. Beggs and P. Fantes, editors. Oxford University Press, Oxford, UK. 212–245.

Pidoux, A.L., S. Uzawa, P.E. Perry, W.Z. Cande, and R.C. Allshire. 2000. Live analysis of lagging chromosomes during anaphase and their effect on spindle elongation rate in fission yeast. *J. Cell Sci.* 113:4177–4191.

Pluta, A.F., A.M. Mackay, A.M. Ainsztein, I.G. Goldberg, and W.C. Earnshaw. 1995. The centromere: hub of chromosomal activities. *Science.* 270:1591–1594.

Polizzi, C., and L. Clarke. 1991. The chromatin structure of centromeres from fission yeast: differentiation of the central core that correlates with function. *J. Cell Biol.* 112:191–201.

Rea, S., F. Eisenhaber, D. O'Carroll, B.D. Strahl, Z.W. Sun, M. Schmid, S. Opravil, K. Mechtler, C.P. Ponting, C.D. Allis, and T. Jenuwein. 2000. Regulation of chromatin structure by site-specific histone H3 methyltransferases. *Nature.* 406:593–599.

Saitoh, S., K. Takahashi, and M. Yanagida. 1997. Mis6, a fission yeast inner centromere protein, acts during G1/S and forms specialized chromatin required for equal segregation. *Cell.* 90:131–143.

Stear, J.H., and M.B. Roth. 2002. Characterization of HCP-6, a *C. elegans* protein required to prevent chromosome twisting and merotelic attachment. *Genes Dev.* 16:1498–1508.

Sugata, N., E. Munekata, and K. Todokoro. 1999. Characterization of a novel kinetochore protein, CENP-H. *J. Biol. Chem.* 274:27343–27346.

Sugata, N., S. Li, W.C. Earnshaw, T.J. Yen, K. Yoda, H. Masumoto, E. Munekata, P.E. Warburton, and K. Todokoro. 2000. Human CENP-H multimers

colocalize with CENP-A and CENP-C at active centromere–kinetochore complexes. *Hum. Mol. Genet.* 9:2919–2926.

Sullivan, B.A., M.D. Blower, and G.H. Karpen. 2001. Determining centromere identity: cyclical stories and forking paths. *Nat. Rev. Genet.* 2:584–596.

Takahashi, K., S. Murakami, Y. Chikashige, H. Funabiki, O. Niwa, and M. Yanagida. 1992. A low copy number central sequence with strict symmetry and unusual chromatin structure in fission yeast centromere. *Mol. Biol. Cell.* 3:819–835.

Takahashi, K., E.S. Chen, and M. Yanagida. 2000. Requirement of Mis6 centromere connector for localizing a CENP-A-like protein in fission yeast. *Science*. 288:2215–2219.

Volpe, T., V. Schramke, G.L. Hamilton, S.A. White, G. Teng, R.A. Martienssen, and R.C. Allshire. 2003. RNA interference is required for normal centromere function. *Chromosome Res*. 11:137–146.

Volpe, T.A., C. Kidner, I.M. Hall, G. Teng, S.I. Grewal, and R.A. Martienssen. 2002. Regulation of heterochromatic silencing and histone H3 lysine-9 methylation by RNAi. *Science*. 297:1833–1837.

Warren, C.D., D.M. Brady, R.C. Johnston, J.S. Hanna, K.G. Hardwick, and F.A. Spencer. 2002. Distinct chromosome segregation roles for spindle checkpoint proteins. *Mol. Biol. Cell.* 13:3029–3041.

Wigge, P.A., and J.V. Kilmartin. 2001. The Ndc80p complex from *Saccharomyces cerevisiae* contains conserved centromere components and has a function in chromosome segregation. *J. Cell Biol.* 152:349–360.

Winey, M., C.L. Mamay, E.T. O'Toole, D.N. Mastronarde, T.H. Giddings, K.L. McDonald, and J.R. McIntosh. 1995. Three-dimensional ultrastructural analysis of the *Saccharomyces cerevisiae* mitotic spindle. *J. Cell Biol.* 129: 1601–1615.

Wood, V., R. Gwilliam, M.A. Rajandream, M. Lyne, R. Lyne, A. Stewart, J. Sgouros, N. Peat, J. Hayles, S. Baker, et al. 2002. The genome sequence of *Schizosaccharomyces pombe*. *Nature.* 415:871–880.

Yu, H.G., and R.K. Dawe. 2000. Functional redundancy in the maize meiotic kinetochore. *J. Cell Biol.* 151:131–142.

The Journal of Cell Biology